frontiers | Frontiers in Earth Science

ORIGINAL RESEARCH
published: 09 June 2022
doi: 10.3389/feart.2022.910666

Links of Hydrogen Sulfide Content With Fluid Components and Physical Properties of Carbonate Gas Reservoirs: A Case Study of the Right Bank of Amu Darya, Turkmenistan

Youyou Cheng[1,2]*, *Zhao Feng*[1], *Chunqiu Guo*[3], *Pengyu Chen*[3], *Chengqian Tan*[1,2], *Haidong Shi*[3] and *Xiang Luo*[1]

[1]*School of Earth Sciences and Engineering, Xi'an Shiyou University, Xi'an, China,* [2]*Shaanxi Key Lab of Petroleum Accumulation Geology, Xi'an, China,* [3]*PetroChina Research Institute of Petroleum Exploration and Development, Beijing, China*

OPEN ACCESS

Edited by:
Wenlong Ding,
China University of Geosciences, China

Reviewed by:
Heng Wang,
Chengdu University of Technology, China
Mingjun Chen,
Southwest Petroleum University, China

***Correspondence:**
Youyou Cheng
charmingx2u@126.com

Specialty section:
This article was submitted to Economic Geology, a section of the journal Frontiers in Earth Science

Received: *04 April 2022*
Accepted: *22 April 2022*
Published: *09 June 2022*

Citation:
Cheng Y, Feng Z, Guo C, Chen P, Tan C, Shi H and Luo X (2022) Links of Hydrogen Sulfide Content With Fluid Components and Physical Properties of Carbonate Gas Reservoirs: A Case Study of the Right Bank of Amu Darya, Turkmenistan. Front. Earth Sci. 10:910666. doi: 10.3389/feart.2022.910666

Hydrogen sulfide (H_2S) in carbonate gas reservoirs shows strong relevance with the natural gas components and has an obvious impact on reservoir types and their petrophysical properties. In this work, core and fluid samples were collected from the Right Bank of Amu Darya reservoirs, Turkmenistan. Then, fluid composition analysis and flash evaporation experiments were performed to investigate the components of reservoir fluid. Petrophysical properties, that is, porosity and permeability, and micropore structures of cores were determined by permeameter–porosimeter and scanning electron microscope (SEM) analysis, respectively. Results in this work indicate that the H_2S content shows obvious relevance to fluid components in carbonate gas reservoirs. With the increase of H_2S content, the total heavy hydrocarbons and potential condensate content decrease, while the condensate density increases. In addition, at higher H_2S content, larger pore and vug porosity was observed. However, in reservoirs with lower H_2S content, the matrix pores are relatively tight and prone to develop fractures. Furthermore, sulfate thermochemical reduction (TSR) is found to be the dominant contributor to high H_2S content in carbonate reservoirs through material and thermodynamic condition analysis. The Gibbs free energy and normalized hydrocarbon content show that the consumption of heavy hydrocarbons generally increases with carbon numbers during TSR, but reaches a minimum at the components of C_7 to C_9. Finally, the relationship between TSR and rock petrophysical properties was discussed, indicating that pore volume enlargement and the dissolution effect of acidic gases are the main mechanisms for TSR to improve carbonate reservoir property. Results in this study present comprehensive analyses of the links between H_2S content and fluid components and petrophysical properties in carbonate gas reservoirs.

Keywords: carbonate gas reservoir, hydrogen sulfide, heavy hydrocarbon, TSR, fracture

1 INTRODUCTION

Currently, carbonate gas reservoirs, accounting for about 45% of the world's total gas reserves, is one of the most significant gas field types (Skrebowski, 1996; Wei et al., 2020). Accompanied by different sizes of pores, fractures, and vugs, carbonate rocks are featured with strong reservoir heterogeneity and anisotropy (Hu et al., 2019; Zhu et al., 2019; Liu D. et al., 2020; Lan et al., 2021; Xue et al., 2021). Hence, carbonate gas reservoirs show significant differences in reservoir characteristics, flow capabilities, and production performances (Cheng et al., 2017; Liu L.-l. et al., 2020; Chen et al., 2021; Zhao et al., 2021). On the other hand, natural gas containing hydrogen sulfide (H_2S) is mostly presented in carbonate reservoirs. Fei et al. (2010) investigated 52 H_2S-bearing oil and natural gas fields all over the world, 48 of which are limestone or dolomite reservoirs. As a consequence, numerous works on the generation and distribution of H_2S and its effect on reservoir features have been done to reveal the relationship between H_2S and the carbonate reservoir (Zhang et al., 2008; He et al., 2019; Liao et al., 2020).

At present, thermal decomposition of sulfur compounds (TDS), bacterial sulfate reduction (BSR), and sulfate thermochemical reduction (TSR) have been regarded as the most significant origins of H_2S in natural gas reservoirs (Basafa and Hawboldt, 2019; Zhao et al., 2019). Due to the toxic effect of H_2S on bacteria, the amount of H_2S from the BSR process is negligible generally (Machel, 2001; Xiao et al., 2021). As for the TDS, the required sulfur compounds such as thiol, thioether, and thiophene are rather scarce in natural gas reservoirs. Besides, the temperature threshold for sufficient thermal decomposition is commonly considered to be not lower than 150°C (Shi and Wu, 2021). Therefore, TSR is regarded as the main contribution to the H_2S in carbonate gas reservoirs (Li et al., 2019; Jia et al., 2021). The favorable conditions of the TSR progress have been widely discussed. In general, the material condition and the thermodynamic condition are believed to be the fundamental preconditions to progress TSR in the underground formation. Morad et al. (2019) concluded that the existence of gypsum rock is the basic precondition to providing sufficient sulfate for TSR. Furthermore, the development of matrix pores, the content of sulfate ions in formation water, formation temperature, gas-water contact, hydrocarbon composition, and so on have been studied on the generation of H_2S (Qu et al., 2019; Liu D. et al., 2020). In addition, Liu et al. (2022) conducted a physical simulation to depict the reaction between anhydrite and organic matters for the generation process of H_2S. Tian et al. (2020) have performed TSR simulations under different temperatures in a closed system to investigate the effect of temperature on the reaction.

The impact of H_2S on the composition of natural gas has been another concerned topic. In the early 1990s, Manzano et al. (1997) noticed the effect of H_2S on oil and gas composition for the first time. Since then, to figure out the component variation of natural gas, a variety of datasets such as petrography, fluid inclusions, and stable isotopes have been used (Deng et al., 2020; Torghabeh et al., 2021). It has been declared that acidic gases like H_2S and CO_2 can increase the drying coefficient of natural gas (Alawi et al., 2020). Up to now, the consumption characteristic of hydrocarbon components during TSR has become the bottleneck for the explanation of the relation between H_2S and hydrocarbon components. Hu et al. (2021) introduced activation energy to distinguish the hydrocarbon loss during TSR and found that the consumption of heavy hydrocarbons would increase along with the carbon numbers. However, the priorities of different hydrocarbon components during the TSR process and the relevance of H_2S content to the fluid components are still unclear.

Actually, the effect of H_2S on the reservoir property should be an integrant part of related research. Some academics have revealed the controlling function of H_2S on the reservoir types and physical properties (Zhao et al., 2019; Liu Y. et al., 2020). Zhang et al. (2005) noticed that the H_2S-rich natural gas is commonly distributed in the porous reservoirs. Cai et al. (2015) declared that the generation of H_2S requires sufficient pore space and connectivity, and the porosity should not be less than 3.5% for H_2S-bearing carbonate reservoirs. From the perspective of TSR, the positive relationship between reservoir porosity and H_2S content has been confirmed by many reports (Mayrhofer et al., 2014; Wu et al., 2022). Accordingly, the good connectedness of the matrix can facilitate the TSR progress for producing H_2S; meanwhile, the metasomatism and dissolution effect of acidic gases can promote the development of high-quality carbonate reservoirs (Lai et al., 2021). Therefore, it is legitimate to declare that TSR plays a positive role in the improvement of carbonate reservoir properties. On basis of this, the study can be furthered by performing a systemic analysis of the pore structure and petrophysical properties of carbonate reservoirs within different H_2S content and figuring out the mechanism involved.

The purpose of this research is to illustrate the links between H_2S content on fluid components and reservoir properties of carbonate gas fields. Core and fluid samples collected from the Right Bank of Amu Darya carbonate reservoirs were used to investigate fluid compositions, microscopic pore structure, and reservoir physical property. Then, the influences of H_2S content on fluid composition and reservoir characteristics were studied in detail. Finally, based on the mechanism of TSR, the priority of hydrocarbon consumption was studied, and its effect on carbonate rock properties was discussed.

2 GEOLOGICAL SETTING

2.1 Fundamental Geological Characteristics

The gas fields of the Right Bank of Amu Darya, Turkmenistan, are located in the northeast portion of the Amu Darya Basin and close to Uzbekistan in the north. It is shaped like a narrow strip and can be divided into six different tectonic units (**Figure 1**). The Callovian–Oxfordian carbonate rocks developed in the Middle–Upper Jurassic Series are the most significant pay zone. The overlying Kimmeridgian–Tithonian Stage is regarded as the giant salt–gypsum formation, with a maximum thickness of 1,600 m (**Figure 2**). The development of salt-gypsum caprocks can provide guarantees for sufficient gas supply and preservation. The sedimentary facies of Callovian–Oxfordian carbonate rocks are

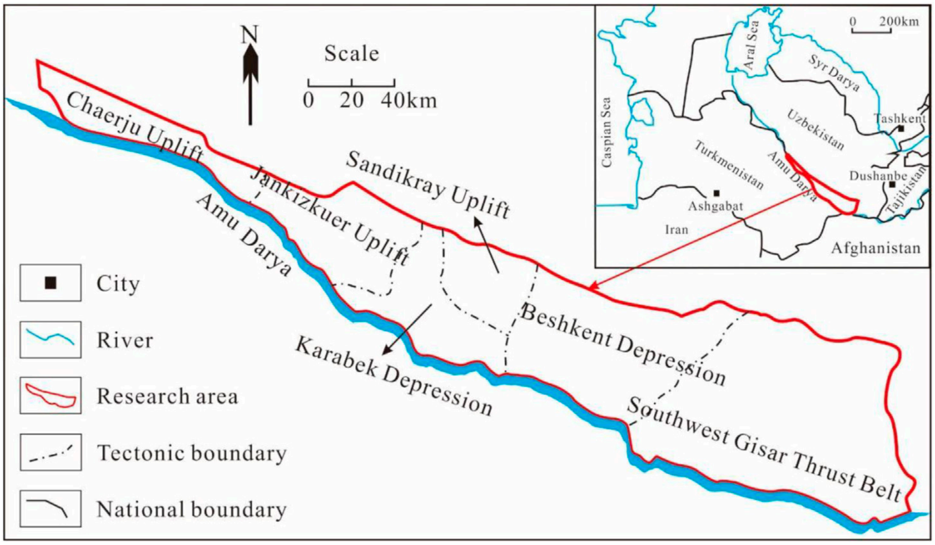

FIGURE 1 | Location of the research area.

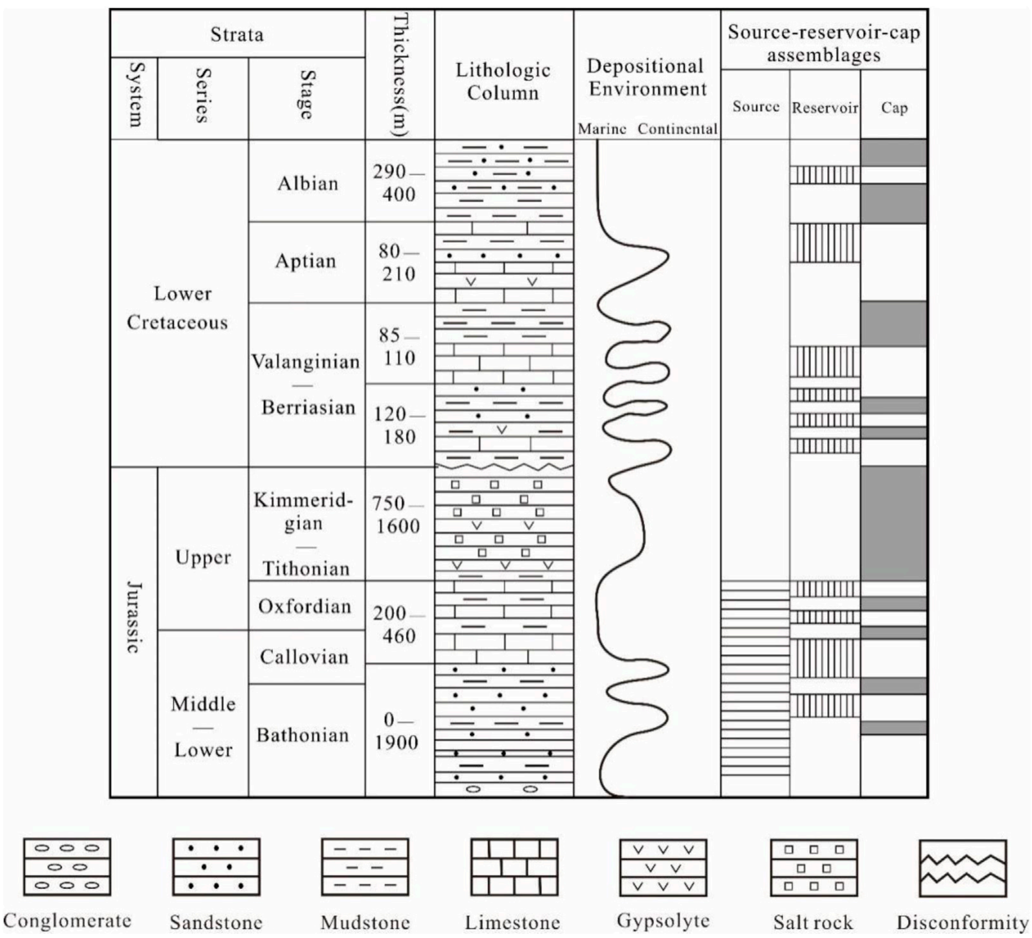

FIGURE 2 | The stratigraphic column of the Right Bank of the Amu Darya reservoirs.

TABLE 1 | H_2S content of different gas fields.

Gas field	H_2S content (%)	Type	Gas field	H_2S content (%)	Type
MJ	5.1084	High H_2S content	YC	0.2903	Low H_2S content
SM	4.2211		UZ	0.0767	
DY	2.0526		KS	0.0541	
YL	0.6254	Medium H_2S content	JR	0.0535	
YJ	0.5048		BP	0.0279	
JD	0.5029		HJ	0.0213	
AK	0.3586		AG	0.0178	
AJ	0.3090		JL	0.0022	

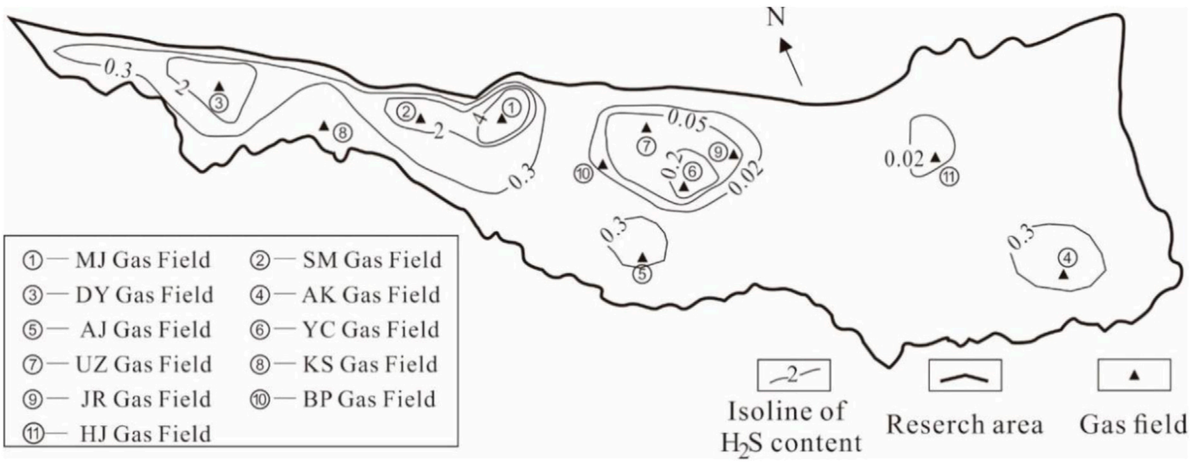

FIGURE 3 | H_2S distribution map of gas fields in the Right Bank of the Amu Darya.

gradually transforming eastward from evaporative platform-open platform to platform margin. Dissolved pores and fractures are widely developed within the reef–shoal bodies.

Currently, sixteen gas fields are being developed in the Right Bank of Amu Darya. All gas fields involved are featured by the marine carbonate reservoir with low porosity and strong heterogeneity. According to core description results, the porosity of the gas fields is 3.43~11.27% in general and 6.37% on average, and permeability is 0.02~18.92 mD in general and 0.77 mD on average. Fractures, especially the high-angled ones, are extensively developed in the pay zone. Reservoir conditions of those gas fields vary notably with the position. Reservoirs in the western region are with large thicknesses and good physical properties with an average porosity of 10%. Conversely, formation thickness decreases for reservoirs in the middle and eastern region, and their flow capability is greatly affected by the natural fractures and vugs.

2.2 H_2S Content

H_2S content of the gas fields of the Right Bank of Amu Darya generally ranges from 0.0022% to 5.1084% (shown in **Table 1**), including classifications of a high content (>2%), medium content (0.3–2%), and low content (<0.3%). **Figure 3** plots the isoline of H_2S content, and it can be observed that gas fields with high H_2S content are distributed in the western regions; while H_2S content of the middle and eastern regions are mostly categorized as medium and low content, especially for reservoirs like BP, HJ, and AG, whose H_2S content are lower than 0.05% in general.

There also exists a certain relation between H_2S content and the burial depth: The H_2S content showed a decreasing trend with the increase of depth. It is the distance from the overlying gypsum rock that provides the explanation for the H_2S content variation with depth. Considering the generation process of H_2S in carbonate reservoirs, the gypsum plays crucial role despite the different reaction mechanisms involved there. As a result, for gas reservoirs in the Right Bank of Amu Darya, the H_2S content experiences an obvious rise with the distance closer to the overlying gypsum rock (**Figure 4**).

3 MATERIALS AND METHODS

3.1 Materials

The gas and condensate samples from 10 reservoirs in the Right Bank of the Amu Darya were collected from the wellhead separator, with an average operating pressure and temperature

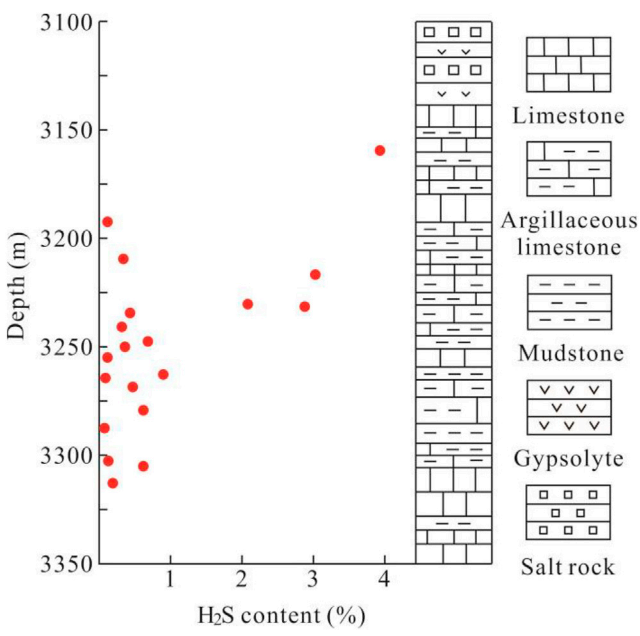

FIGURE 4 | The relation between H_2S content and the burial depth.

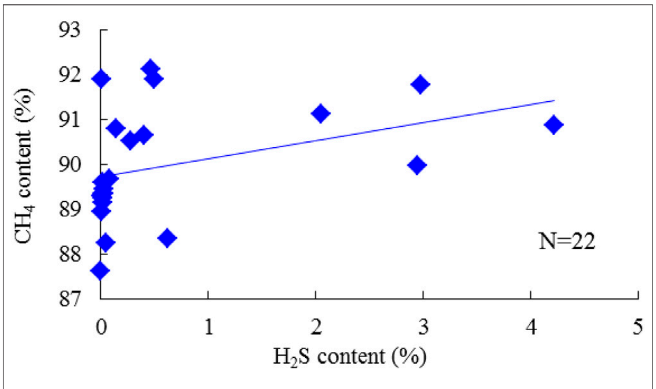

FIGURE 5 | Relationship between CH_4 and H_2S content.

of 1.82 MPa and 32°C, respectively. All fluid samples were immediately sealed into sampling bottles to avoid component loss. Basic information and properties of the gas and condensate samples are shown in **Table 2**. To characterize the petrophysical properties and microscopic pore structure of the reservoir rocks, ten core samples were collected, with three cores from the western region and the rest from the middle and east.

3.2 Experimental Methods

3.2.1 Fluid Composition Analysis

The composition of gas and condensate samples was analyzed by the chromatograph Agilent 7890A, abiding by the Industrial Standard "Analysis of natural gas composition: Gas chromatographic method (GB/T 13610-2014)." The hydrocarbons were determined from methane (C_1) to icosane (C_{20}) for the gas samples and from C_1 to tetratriacontane (C_{34}) for the condensate, respectively. The main nonhydrocarbon components, referring to H_2S, nitrogen (N_2), and carbon dioxide (CO_2), were also detected. Each component was expressed with its mole fraction in the gas and condensate sample.

3.2.2 Flash Evaporation Experiment

Flash evaporation experiments of the condensate samples were performed at the standard temperature and pressure using a flash tank to separate flash gas and volatile oil from the condensate. The gas–oil ratio (GOR) and formation volume factor (FVF) of the condensate and the composition of the gas, flash gas, and volatile oil were determined. Then, the well production fluid components under formation conditions were calculated following the "Test method for reservoir fluid physical properties (GB/T 26981-2011)."

3.2.3 Core Sample Analysis

The porosity of the core samples was measured based on Boyle–Mariotte's law *via* a Core Porosimeter OFITE 350, while, an *in situ* N_2 displacement experiment was launched to obtain the Klinkenberg permeability of the core with a core flooding device STL-II. All the test procedures abide by the "Core Analysis Method (SY/T 5336-2019)." Furthermore, the ultrahigh resolution scanning electron microscope (SEM) device QUANTA 400 was involved to characterize the structure of the pores and microfractures within the gold-coated core slice.

4 EXPERIMENTAL RESULTS

4.1 Relationships Between Fluid Component With H_2S Content

4.1.1 Hydrocarbon Components

Methane (CH_4) is the dominant component of natural gas. The measured CH_4 content varies from 87.617% to 92.779%, with an average of 95.308% in the gas phase. The cross-plot of CH_4 and H_2S content was plotted to investigate their relationships, as shown in **Figure 5**. However, the positive correlation is weak. Heavy hydrocarbons, that is, the C_{2+} component, mainly appear in the condensate phase; for gas and condensate samples, the C_{2+} content

TABLE 2 | Basic information and physical properties of samples.

Type	Formation information			Operating condition			Sample property	
	Depth (m)	Pressure (MPa)	Temperature (°C)	Sampling position	Pressure (MPa)	Temperature (°C)	Numbers	Relative density
Gas	3,150–3,570	53–62	107–121	Wellhead separator	0.45–3.46; 1.82 average	24–36; 32 average	22	0.64
Condensate							22	0.78

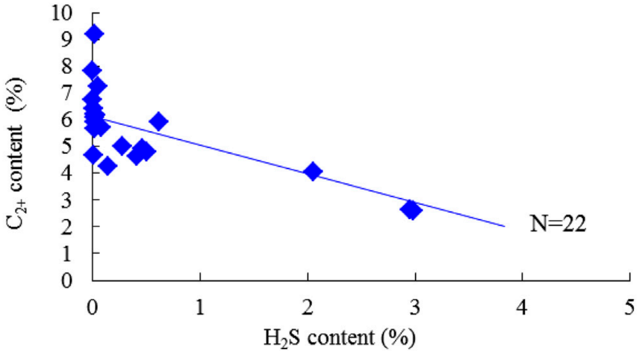

FIGURE 6 | Relationship between C_{2+} and H_2S content.

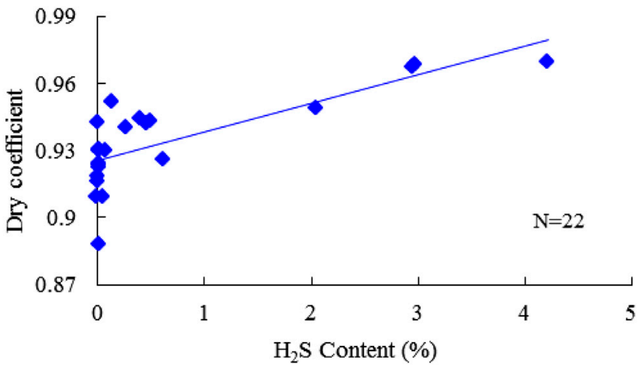

FIGURE 7 | Relationship between dry coefficient and H_2S content.

was 4.459% and 87.984%, respectively. The C_{2+} content generally presents a negative correlation with the increase of H_2S content, especially for samples with medium and high H_2S content (**Figure 6**). Correspondingly, the dry coefficient, referring to the ratio of the CH_4 content to the C_{2+} content in natural gas, shows a positive trend with the H_2S content (**Figure 7**).

To investigate the relationship between condensate and H_2S content, the potential condensate contents were calculated from the flash evaporation results of the well production fluids. The potential content decreases and the density increases with the H_2S content as shown in **Figure 8**, indicating that the heavy hydrocarbons could act as reactants in the production of H_2S, but their consumption would not increase monotonously with the carbon number.

4.1.2 Nonhydrocarbon Components

N_2 is relatively scarce in the Right Bank of Amu Darya and its content varies slightly within the limit of 0.271%–0.516% in the well production fluid. The studied gas fields can be defined as medium CO_2 content reservoirs, whose content ranges from 0.917% to 4.556%, according to "The classification of the gas pool (SY/T 6168-2009)." As shown in **Figure 9**, CO_2 content is independent of H_2S at low and medium content ranges, while a positive correlation can be found between CO_2 and H_2S at high H_2S content. In addition, CO_2 content is greater than H_2S content within all samples despite the H_2S degree.

4.2 Reservoir Characteristics With H_2S Content

4.2.1 Porosity and Permeability

Similar to most carbonate reservoirs with fractures, the porosity and permeability of studied reservoirs do not show a clear positive correlation (**Figure 10**). As shown in **Figure 11**, the porosity increases with the increase of H_2S content, and the same trend can be found for the permeability of core samples without fractures. However, for core samples with fractures, there is no clear correlation observed between permeability and H_2S content as permeability is mainly affected by fractures. Actually, due to the lower aperture and higher permeability of fractures, the Poro–Perm Relation would somehow overturn in fractured reservoirs, which explains the differences in porosity and permeability with H_2S content. Therefore, porosity should be an intrinsic factor to figure out the effect of H_2S on reservoir physical properties.

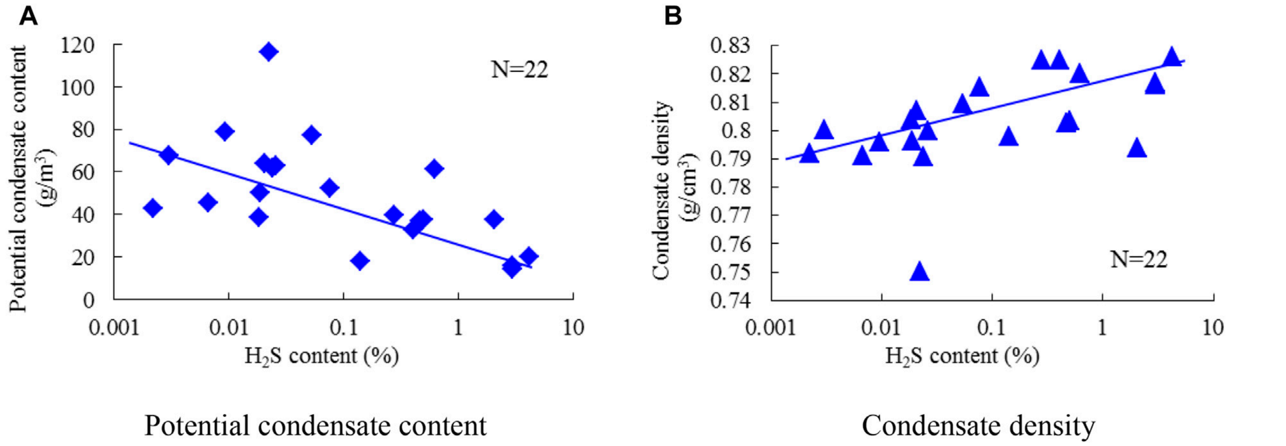

FIGURE 8 | Relationship between condensate property and H_2S content. **(A)** Potential condensate content. **(B)** Condensate density.

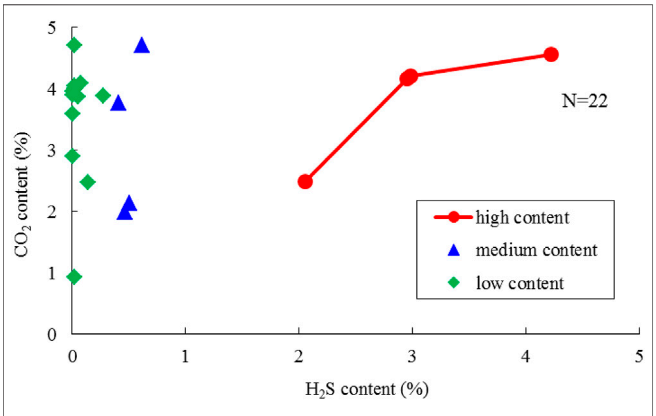

FIGURE 9 | Relationship between CO_2 and H_2S content.

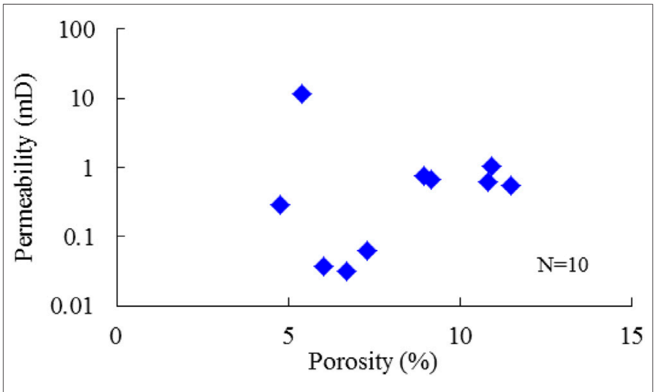

FIGURE 10 | Porosity and permeability of core samples.

4.2.2 Reservoir Types

The Right Bank of Amu Darya experienced multistage tectonic movement, and a large number of structural fractures were generated during that process. Meanwhile, the dissolution of the carbonate rocks caused by acidic gases can result in a large number of dissolved pores and vugs. As a consequence, diverse reservoir types have been discriminated in this area, among which pore, pore-fracture, pore-vug, and fracture are the most representative types.

The SEM analysis facilitates the connections between H_2S and reservoir microstructures. As can be seen in **Figure 12**: 1) Well DY-21, whose H_2S content was measured to be 2.0526%, was classified as the pore-vug type. The porosity and permeability were 11.47% and 0.55 mD, respectively. The SEM slice can observe a distinct moldic vug associated with the primary pores. 2) Well AJ-21, whose H_2S content was measured to be 0.3090%, was classified as the pore type. The porosity and permeability were 7.31% and 0.062 mD, respectively. The pore structure showed great homogeneity and intercrystal pores were commonly distributed. 3) BL-22 well, whose H_2S content was measured to be 0.0279%, was classified as the pore-fracture type. The porosity and permeability were 6.41% and 11.64 mD, respectively. The SEM slice was penetrated by a dissolved fracture, while the surrounding pores in the matrix are rather tight. This indicates that the H_2S could be regarded as one of the evidence to characterize the reservoir property for the gas fields in the Right Bank of Amu Darya. With higher H_2S content, the porosity would be larger and the reservoir types mainly consist of pore and pore-vug. Yet, for reservoirs with low H_2S content, the matrix pore could be relatively tight and prone to develop with fractures.

To further expand this knowledge, H_2S content, porosity, and brief reservoir descriptions of 10 major gas fields from different regions of the Right Bank of Amu Darya are summarized in **Table 3**. It shows that gas fields in the western region can be characterized as high H_2S content and high porosity reservoirs. However, H_2S content rarely exceeds 0.07% in the middle and east where fractures are well developed. In particular, for gas field JL with H_2S content of 0.0022%, the porosity almost reaches the lower limit of the effective pore, and the field is thus defined as a pure fractured reservoir.

5 DISCUSSION

5.1 H_2S Origin of Gas Fields in the Right Bank of Amu Darya

With respect to the TDS and BSR, TSR has been regarded as the most significant H_2S origin. TSR refers to a series of reduction reactions between sulfates and hydrocarbons, and the sulfates are consequently reduced into acidic gases, that is,

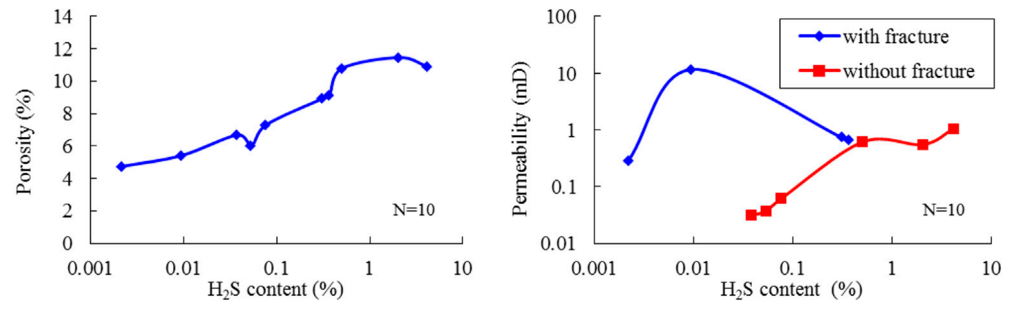

FIGURE 11 | Relationship between reservoir physical properties and H_2S contents.

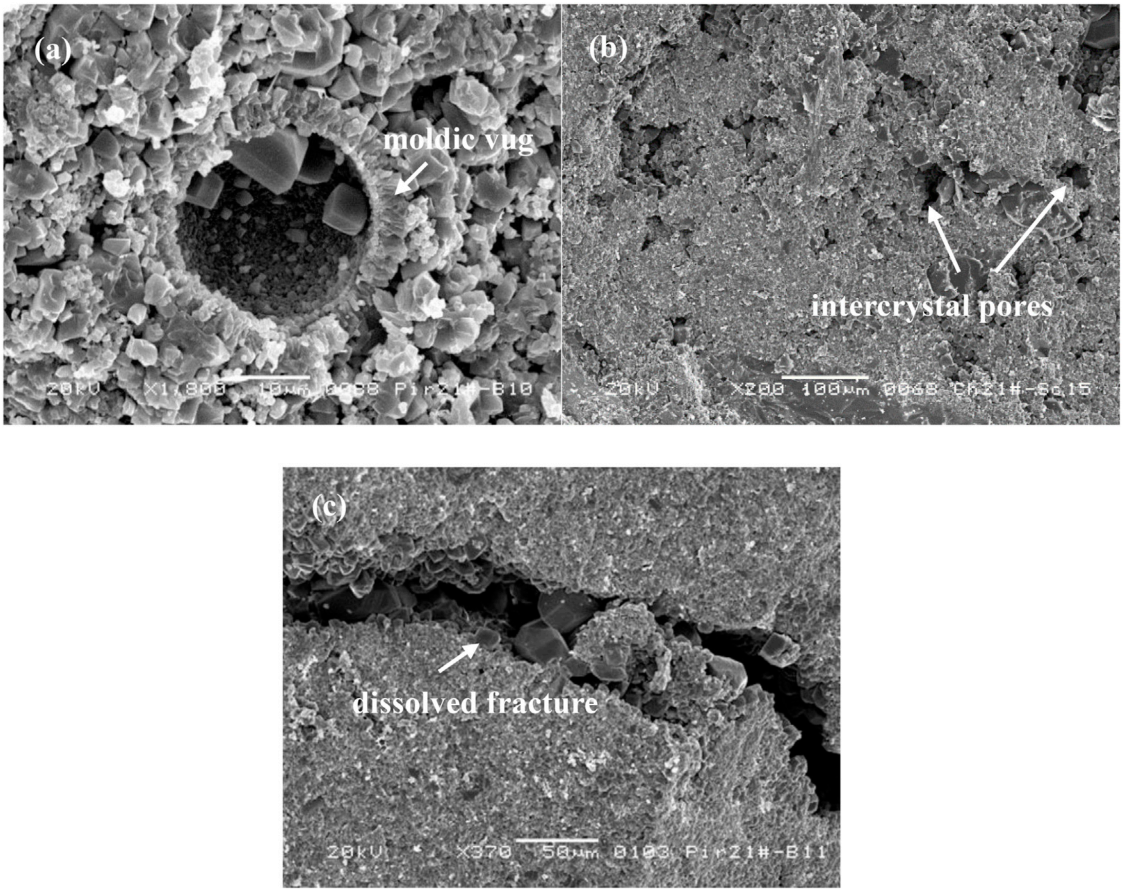

FIGURE 12 | The SEM images of core samples. **(A)** Well DY-21, showing a moldic vug; **(B)** Well AJ-21, developing with intercrystal pores; **(C)** BL-22 Well, showing a dissolved fracture.

TABLE 3 | H_2S content and reservoir characteristics of typical fields.

Gas field	Region	H_2S content (%)	Porosity (%)	Reservoir description	Reservoir type
DY	West	2.0526	9.27–13.66	Brownish gray silty limestone, light gray micritic limestone; primary pores are well developed, along with subsize vugs	Pore-vug
SM	West	4.2211	8.89–14.85	Brownish gray limestone, fine quality; the whole reservoir is of good physical properties with medium–high porosity	Pore-vug
JD	West	0.5029	9.37–12.81	Light gray silty dolomite, with good physical properties	Pore
YJ	Middle	0.5048	7.46–11.16	Light gray silty limestone; high porosity and permeability, low water saturation	Pore-vug
BP	Middle	0.0279	4.61–9.81	Dark gray and brownish gray micritic limestone, with high fracture development degree	Pore-fracture
UZ	Middle	0.0767	6.37–10.13	Grayish brown and light gray micritic limestone or silty limestone; microfractures are well developed	Pore-fracture
JR	Middle	0.0535	5.72–7.53	Brownish gray silty limestone; high angle fractures are developed	Pore-fracture
AJ	Middle	0.3090	8.62–9.93	Light gray bioclastic limestone; dissolved fracture pores and vugs are developed	Pore-vug
AG	East	0.0178	5.16–7.03	Brownish gray silty limestone; medium-scale fractures intensively are developed	Pore-fracture
JL	East	0.0022	3.53–5.04	Gray, brownish-gray micritic limestone; tight matrix pores, fractures are well developed	Fracture

H_2S and CO_2. The reaction process can be summarized in **Eq. 1** (Zhang et al.,2008; He et al., 2019):

$$C_n\mathrm{H}_{2n+2} + n\mathrm{CaSO}_4 \rightarrow n\mathrm{CaCO}_3 + \mathrm{H}_2\mathrm{S} + n\mathrm{H}_2\mathrm{O} \pm \mathrm{CO}_2 \pm \mathrm{S} \quad (1)$$

It is generally believed that the TSR requires the following preconditions: hydrocarbons, sulfate (material conditions), and high temperature (thermodynamic condition). Because the TSR can hardly advance with the anhydrite, the reaction rate depends on the dissolution of calcium sulfate ($CaSO_4$) in the formation water. Therefore, higher connectivity is essential to allow adequately mixing between dissolved sulfate with hydrocarbons.

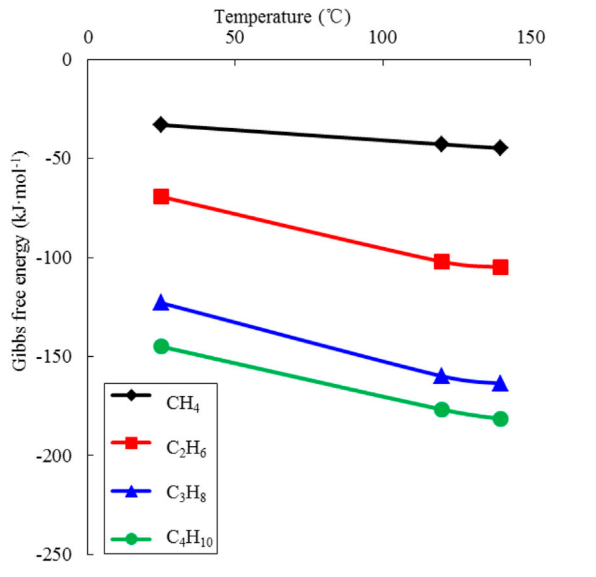

FIGURE 13 | The Gibbs free energy of C_2H_6 to C_4H_{10} during TSR at different temperatures.

For the carbonate gas reservoirs in the Right Bank of Amu Darya, the material conditions, that is, hydrocarbons and sulfate, have undoubtedly met the requirement of TSR. Furthermore, the overlying gypsum-salt rock and the interbedded limestone-gypsum layers, dispersing in the upper section of the Callovian-Oxfordian Stage, provide direct contact for hydrocarbons and $CaSO_4$ to complete the reaction in the pay zone. The current formation temperature of the Amu Darya Basin ranges from 100 to 130°C. In view of the tectonic movement in the Himalayan period, the formation experienced higher temperatures. According to the inclusions homogenization temperature, the paleo–geotemperature of the reservoir had once reached 140°C, which exceeds the temperature threshold of TSR. Therefore, TSR is the dominant origin of H_2S in carbonate gas reservoirs in the Right Bank of Amu Darya. Ma et al. (2021) confirm that TSR is the principal producer of H_2S in the Right Bank of Amu Darya and also the contributor to the development of secondary pores.

5.2 Hydrocarbon Consumptions in the TSR Process

To clarify the relation between hydrocarbons and H_2S content, the priority of different hydrocarbon components involved in the TSR should be studied. According to the Van't Hoff isothermal formula (Atkins and De, 2006), the Gibbs free energy of each component can be determined with **Eq. 2**.

$$\Delta_r G_{\mathrm{m}} = \Delta_r G_{\mathrm{m}}^{\Theta} + RT \ln Q \tag{2}$$

where $\Delta_r G_{\mathrm{m}}$ is the Gibbs free energy, kJ/mol; $\Delta_r G_{\mathrm{m}}^{\Theta}$ is the standard formation free energy at 298.15 K, kJ/mol; R is the thermodynamic constant, 8.314 J/(mol·K); T is the reaction temperature, K; Q is the reaction quotient.

Figure 13 shows the calculated Gibbs free energy of CH_4 to C_4H_{10} involved in TSR at different temperatures. It can be seen that: 1) The Gibbs free energy is decreasing dramatically with the increased temperature, which elucidates the necessity of high temperature for activating the reaction. 2) The Gibbs free energy of CH_4 stays at a high level despite the rising temperature, indicating that CH_4 is difficult to participate in the TSR reaction. This coincides with the statement mentioned in **Section 4.1** that "no clear relation observed between CH_4 and H_2S content." 3) For heavy hydrocarbons from C_2H_6 to C_4H_{10}, all calculated Gibbs free energy are less than −100 kJ/mol at the temperature of 120–140 °C, which demonstrates that these components are available in TSR at the reservoir conditions. In addition, the Gibbs free energy decreases with the increase of carbon numbers, indicating a rising trend of the consumption from C_2H_6 to C_4H_{10}.

Furthermore, to investigate the relative decrement of each hydrocarbon component along with per unit H_2S content growth, the normalized hydrocarbon content was used in this study. With well production fluid composition given, regressions between the normalized content of each hydrocarbon component and the H_2S content can be established. The correlation slope can thus be employed to describe the consumption involved in TSR. Considering that the slope showed a negative value, the absolute value of the slope was adopted and named the "relative consumption." The definition of the normalized content and the regression results for each component is attached in **Supplementary Appendix**.

The relative consumptions of different heavy hydrocarbon components are shown in **Figure 14**. It was found that there is a V-shaped relationship between relative consumption and carbon number. The consumptions reach the minimum value at C_7 and then increase with carbon numbers; as a consequence, the consumptions of C_7 to C_9 are relatively low among all heavy hydrocarbon components except for C_2. This provides a reasonable interpretation for the variation of condensate content and density with H_2S content. The decrease of potential condensate content is caused by the consumption of total heavy hydrocarbons; while the remnant of intermediate components, typified by C_7 to C_9, would lead to an increase in condensate density.

To sum up, heavy hydrocarbons act as the reactant in TSR, while CH_4 can hardly take part in the reaction. The consumption of heavy hydrocarbons generally increases with carbon numbers but reaches a minimum at C_7~C_9. The relative consumption method facilitates the reveal of hydrocarbon consumption and explains the dynamic of gas and condensate features with H_2S content.

5.3 Influence of TSR on Nonhydrocarbon Components

As mentioned earlier, inert gases like N_2 are merely affected by H_2S content, whereas the CO_2 content shows a positive correlation with H_2S content at higher concentrations. This is because CO_2 is also one of the products of TSR. In addition, H_2S dissolution in formation water can form hydrosulfuric acid, which will further react with carbonate minerals to produce CO_2. It explains the content of CO_2 is higher than that of H_2S, which can be regarded as one of the symbols of carbonate reservoirs emerging TSR.

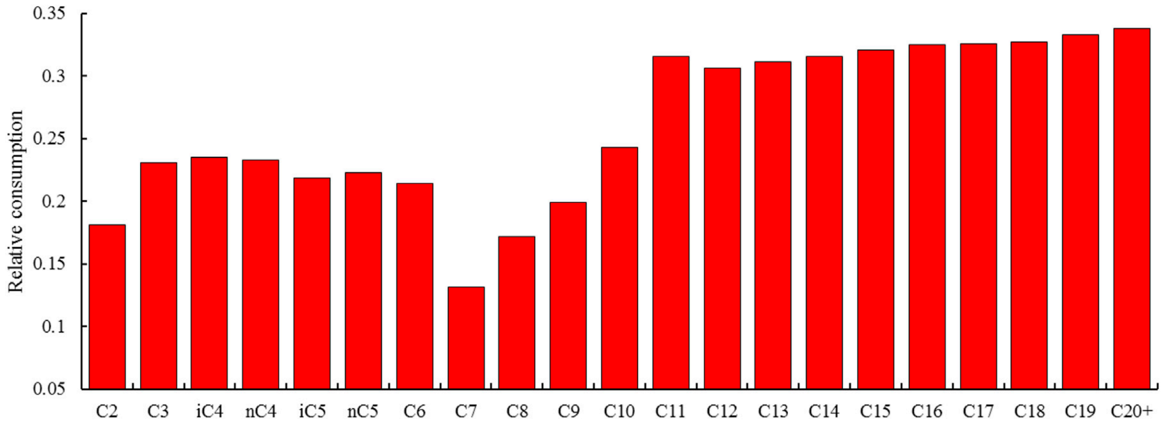

FIGURE 14 | The relative consumption of heavy hydrocarbon components in TSR.

5.4 Improvement of Reservoir Property Through TSR

From the perspective of TSR, the contribution of H_2S to the improvement of porosity can then be discerned. The controlling factor of TSR on reservoir physical properties and reservoir types can be manifested in the following aspects:

1) Compared to the fractured reservoirs, pore and pore-vug typed reservoirs are of higher connectedness and larger storage capacity, which not only provide space for the mutual contact of the reactants but also ensure a continuous supply of reactants and transfer of products. This prompts the TSR in the right direction. It explains why H_2S-bearing natural gas fields are generally discovered in large porous reservoirs.
2) It can be noticed from **Eq. 1** that 1 mol of calcite ($CaCO_3$) can be generated with 1 mol of anhydrite ($CaSO_4$). The molar volume of $CaCO_3$ and $CaSO_4$ are 37 cm^3/mol and 47 cm^3/mol, respectively. Therefore, after 1 mol of anhydrite is involved in the reaction, the pore volume of the reservoir rock would increase by about 10 cm^3. This process is usually called the "pore volume enlargement" effect of the TSR.
3) As the products of TSR, large amounts of H_2S and CO_2, which are acidic gases and soluble in formation water, played a significant role in the growth of secondary pores and vugs in carbonate rock. It is also an important mechanism to improve the porosity of carbonate reservoirs.

6 CONCLUSION

1) The H_2S content shows obvious relevance to fluid components in carbonate gas reservoirs. With the increase of H_2S content, the total content of heavy hydrocarbons decreases, causing the reduction of potential condensate content, while the condensate density is increasing with the H_2S content. In high H_2S content reservoirs, a positive correlation was observed between CO_2 content and H_2S content.
2) With higher H_2S content, the porosity would be larger and the reservoir rock mainly consists of pores and vugs; while for reservoirs with low H_2S content, the matrix pores could be relatively tight and prone to develop with fractures.
3) TSR is the dominant hydrogen sulfide origin for H_2S-rich carbonate reservoirs resembling the Right Bank of Amu Darya. The consumption of heavy hydrocarbons during TSR generally increases with carbon numbers but would reach a minimum at the components of C_7 to C_9. The pore volume enlargement and the dissolution effect of acidic gases can be regarded as the main mechanisms for the improvement of the reservoir property of TSR.

DATA AVAILABILITY STATEMENT

The raw data supporting the conclusion of this article will be made available by the authors, without undue reservation.

AUTHOR CONTRIBUTIONS

YC is responsible for the idea and writing of the manuscript; ZF, PC, CT, and HS are responsible for the experiments; CG and XL are responsible for the analysis and interpretation of data.

FUNDING

This work is financially supported by the Scientific Research and Technology Development Project of CNPC (2021DJ3301) and the General Special Scientific Research Plan of the Shaanxi Provincial Department of Education (20JK0848).

SUPPLEMENTARY MATERIAL

The Supplementary Material for this article can be found online at https://www.frontiersin.org/articles/10.3389/feart.2022.910666/full#supplementary-material

REFERENCES

Atkins, P., and De, P. J. (2006). *Physical Chemistry 8th*. New York: W.H. Freeman and Company.

Ba Alawi, M., Hassan, A., Aljawad, M. S., Kamal, M. S., Mahmoud, M., and Al-Nakhli, A. (2020). A Novel Approach to Improve Acid Diversion in Carbonate Rocks Using Thermochemical Fluids: Experimental and Numerical Study. *Molecules* 25, 2976. doi:10.3390/molecules25132976

Basafa, M., and Hawboldt, K. (2019). Reservoir Souring: Sulfur Chemistry in Offshore Oil and Gas Reservoir Fluids. *J. Petrol Explor Prod. Technol.* 9, 1105–1118. doi:10.1007/s13202-018-0528-2

Cai, C., Hu, G., Li, H., Jiang, L., He, W., Zhang, B., et al. (2015). Origins and Fates of H_2S in the Cambrian and Ordovician in Tazhong Area: Evidence from Sulfur Isotopes, Fluid Inclusions and Production Data. *Mar. Petroleum Geol.* 67, 408–418. doi:10.1016/j.marpetgeo.2015.05.007

Chen, G. B., Li, T., Yang, L., Zhang, G. H., Li, J. W., and Dong, H. J. (2021). Mechanical Properties and Failure Mechanism of Combined Bodies with Different Coal-Rock Ratios and Combinations. *J. Min. Strata Control Eng.* 3 (2), 023522. doi:10.13532/j.jmsce.cn10-1638/td.20210108.001

Cheng, Y., Mu, L., Zhu, E., Zhang, P., Guo, C., Leng, Y., et al. (2017). Water Producing Mechanisms of Carbonate Reservoirs Gas Wells: A Case Study of the Right Bank Field of Amu Darya, Turkmenistan. *Petroleum Explor. Dev.* 44, 89–96. doi:10.1016/s1876-3804(17)30011-3

Deng, Q., Zhang, T., Zhao, F., Wang, H., and Yin, J. (2020). The Influence of Hydrogeology to Generation of Hydrogen Sulfide of Low-Rank Coal in the Southeast Margin of Junggar Basin, China. *Geofluids* 2020, 1–10. doi:10.1155/2020/8859100

Fei, A. G., Zhu, G. Y., Zhang, S., Hu, J., Chen, S., Zhang, B., et al. (2010). Global Distribution Hydrogen Sulphide-Bearing Natural Gas and the Major Factors Controlling its Formation. *Earth Sci. Front.* 17, 350–360. doi:10.3724/SP.J.1231.2010.06586

He, K., Zhang, S., Mi, J., Ma, Q., Tang, Y., and Fang, Y. (2019). Experimental and Theoretical Studies on Kinetics for Thermochemical Sulfate Reduction of Oil, C2-5 and Methane. *J. Anal. Appl. Pyrolysis* 139, 59–72. doi:10.1016/j.jaap.2019.01.011

Hu, A., Shen, A., Yang, H., Zhang, J., Wang, X., Yang, L., et al. (2019). Dolomite Genesis and Reservoir-Cap Rock Assemblage in Carbonate-Evaporite Paragenesis System. *Petroleum Explor. Dev.* 46, 969–982. doi:10.1016/S1876-3804(19)60253-3

Hu, Y., Cai, C., Liu, D., Peng, Y., Wei, T., Jiang, Z., et al. (2021). Distinguishing Microbial from Thermochemical Sulfate Reduction from the Upper Ediacaran in South China. *Chem. Geol.* 583, 120482. doi:10.1016/j.chemgeo.2021.120482

Jia, L., Cai, C., Zhang, J., Liu, L., Luo, Q., and Li, K. (2021). Effect of Thermochemical Sulfate Reduction on Carbonate Reservoir Quality: Cambrian and Ordovician Oilfield, Tazhong Area, Tarim Basin, China. *Mar. petroleum Geol.* 123, 104745. doi:10.1016/j.marpetgeo.2020.104745

Lai, J., Liu, S., Xin, Y., Wang, S., Xiao, C., Song, Q., et al. (2021). Geological-petrophysical Insights in the Deep Cambrian Dolostone Reservoirs in Tarim Basin, China. *Bulletin* 105, 2263–2296. doi:10.1306/03122119135

Lan, S. R., Song, D. Z., Li, Z. L., and Liu, Y. (2021). Experimental Study on Acoustic Emission Characteristics of Fault Slip Process Based on Damage Factor. *J. Min. Strata Control Eng.* 3 (3), 033024. doi:10.13532/j.jmsce.cn10-1638/td.20210510.002

Li, K., George, S. C., Cai, C., Gong, S., Sestak, S., Armand, S., et al. (2019). Fluid Inclusion and Stable Isotopic Studies of Thermochemical Sulfate Reduction: Upper Permian and Lower Triassic Gasfields, Northeast Sichuan Basin, China. *Geochimica cosmochimica acta* 246, 86–108. doi:10.1016/j.gca.2018.11.032

Liao, J., Wang, T., Lu, H., Greenwood, P. F., Peng, P. a., and Samuel Hsu, C. (2020). Effects of Mississippi Valley-type Minerogenetic Metal Sulfates on Thermochemical Sulfate Reduction, Studied by Hydrous Pyrolysis. *Org. Geochem.* 150, 104128. doi:10.1016/j.orggeochem.2020.104128

Liu, D., Li, J., Liu, J.-q., and Zhang, L. (2020). Modeling Hydrocarbon Accumulation Based on Gas Origin and Source Rock Distribution in Paleozoic Strata of the Ordos Basin, China. *Int. J. Coal Geol.* 225, 103486. doi:10.1016/j.coal.2020.103486

Liu, L.-l., Cui, Z.-h., Wang, J.-j., Xia, Z.-h., Duan, L.-j., Yang, Y., et al. (2020). Pore Size Distribution Characteristics of High Rank Coal with Various Grain Sizes. *ACS Omega* 5, 19785–19795. doi:10.1021/acsomega.0c02569

Liu, Y., Gao, M., and Zhao, H. (2020). Detection of Overlying Rock Structure and Identification of Key Stratum by Drilling and Logging Technology. *J. Min. Strata Control Eng.* 2 (2), 023038. doi:10.13532/j.jmsce.cn10-1638/td.2020.02.004

Liu, Y., Zhang, C., Ding, K., Yu, Z., and Wu, Y. (2022). Thermochemical Sulfate Reduction by Pyrobitumen: Review and Experiments. *ACS Earth Space Chem.* 6, 308–321. doi:10.1021/acsearthspacechem.1c00291

Ma, W. X., Ou, C. Y., Liao, Y. B., Xu, Q. K., Chen, R. J., Wang, X., et al. (2021). Characteristics and Genesis of Oxford Stage Microbial Limestone Reservoir in Eastern Amu Darya Basin. *Lithol. Reserv.* 33 (5), 59–69. doi:10.12108/yxyqc.20210506

Machel, H. G. (2001). Bacterial and Thermochemical Sulfate Reduction in Diagenetic Settings — Old and New Insights. *Sediment. Geol.* 140 (1), 143–175. doi:10.1016/S0037-0738(00)00176-7

Manzano, B. K., Fowler, M. G., and Machel, H. G. (1997). The Influence of Thermochemical Sulphate Reduction on Hydrocarbon Composition in Nisku Reservoirs, Brazeau River Area, Alberta, Canada. *Org. Geochem.* 27, 507–521. doi:10.1016/S0146-6380(97)00070-3

Mayrhofer, C., Niessner, R., and Baumann, T. (2014). Hydrochemistry and Hydrogen Sulfide Generating Processes in the Malm Aquifer, Bavarian Molasse Basin, Germany. *Hydrogeol. J.* 22, 151–162. doi:10.1007/s10040-013-1064-2

Morad, D., Nader, F. H., Morad, S., Rossi, C., Gasparrini, M., Alsuwaidi, M., et al. (2019). Limited Thermochemical Sulfate Reduction in Hot, Anhydritic, Sour Gas Carbonate Reservoirs: The Upper Jurassic Arab Formation, United Arab Emirates. *Mar. petroleum Geol.* 106, 30–41. doi:10.1016/j.marpetgeo.2019.04.023

Qu, X., Chen, S., Yang, X., You, L., and Zhong, J. (2019). Study on Hydrocarbon Accumulation Period in Deep Water Areas of the South China Sea: An Example from the Miocene Reservoir of the Ledong-Lingshui Sag in the Qiongdongnan Basin. *J. Coast. Res.* 94, 112–116. doi:10.2112/SI94-021.1

Shi, Q., and Wu, J. (2021). Review on Sulfur Compounds in Petroleum and its Products: State-Of-The-Art and Perspectives. *Energy fuels.* 35 (18), 14445–14461. doi:10.1021/acs.energyfuels.1c02229

Skrebowski, C. (1996). *World Oilfields and World Gasfields Series*. South America: The Petroleum Economist Ltd.

Tian, J., Li, J., Kong, H., Zeng, X., Wang, X., Dong, L., et al. (2021). Genesis of Hydrogen Sulfide in Natural Gas Reservoirs in the Western Qaidam Basin. *Interpretation* 9, T223–T233. doi:10.1190/INT-2020-0120.1

Torghabeh, A. K., Kalantariasl, A., Kamali, M., and Akbarifard, M. G. (2021). Reservoir Gas Isotope Fingerprinting and Mechanism for Increased H2S: An Example from Middle East Shanul Gas Field. *J. petroleum Sci. Eng.* 199, 108325. doi:10.1016/j.petrol.2020.108325

Wei, G., Du, J., Zou, C., Xu, C., Yang, W., Xie, W., et al. (2020). The Anyue Giant Gas Field in the Sichuan Basin as the Largest Gas Field in Marine Carbonate Deposits from Domestic China. *Russ. Geol. Geophys.* 61, 1015–1027. doi:10.15372/RGG2020127

Wu, X. L., Xu, W. L., Li, R. X., Li, N. X., Liu, Q., Zhao, D., et al. (2022). Genesis of Hydrogen Sulfide in Ordovician Majiagou Formation ,mid-Eastern Ordos Basin:evidence from Fluid Inclusions[J]. *Acta Pet. Sin.* 43 (2), 250–261. doi:10.7623/syxb202202007

Xiao, Q., Cai, S., and Liu, J. (2021). Microbial and Thermogenic Hydrogen Sulfide in the Qianjiang Depression of Jianghan Basin: Insights from Sulfur Isotope and Volatile Organic Sulfur Compounds Measurements. *Appl. Geochem.* 126, 104865. doi:10.1016/j.apgeochem.2020.104865

Xue, F., Liu, X. X., and Wang, T. Z. (2021). Research on Anchoring Effect of Jointed Rock Mass Based on 3D Printing and Digital Speckle Technology. *J. Min. Strata Control Eng.* 3 (2), 023013. doi:10.13532/j.jmsce.cn10-1638/td.20201020.001

Zhang, S. C., Zhu, G. Y., Dai, J. X., Xiong, Y., and Liang, Y. B. (2005). TSR and Sour Gas Accumulation: A Case Study in the Sichuan Basin, SW China. *Geochimica Cosmochimica Acta* 69, 562. doi:10.1016/j.gca.2005.03.033

Zhang, S., Shuai, Y., and Zhu, G. (2008). TSR Promotes the Formation of Oil-Cracking Gases: Evidence from Simulation Experiments. *Sci. China Ser. D-Earth Sci.* 51, 451–455. doi:10.1007/s11430-008-0009-4

Zhao, H., Liu, W., Borjigin, T., Zhang, J., Luo, H., and Wang, X. (2019). Study of Thermochemical Sulfate Reduction of Different Organic Matter: Insight from Systematic TSR Simulation Experiments. *Mar. Petroleum Geol.* 100, 434–446. doi:10.1016/j.marpetgeo.2018.11.009

Zhao, K. K., Jiang, P. F., Feng, Y. J., Sun, X. D., Cheng, L. X., and Zheng, J. W. (2021). Investigation of the Characteristics of Hydraulic Fracture Initiation by Using Maximum Tangential Stress Criterion. *J. Min. Strata Control Eng.* 3 (2), 023520. doi:10.13532/j.jmsce.cn10-1638/td.20201217.001

Zhu, D., Liu, Q., Zhang, J., Ding, Q., He, Z., and Zhang, X. (2019). Types of Fluid Alteration and Developing Mechanism of Deep Marine Carbonate Reservoirs. *Geofluids* 2019, 1–18. doi:10.1155/2019/3630915

Conflict of Interest: The authors declare that the research was conducted in the absence of any commercial or financial relationships that could be construed as a potential conflict of interest.

Publisher's Note: All claims expressed in this article are solely those of the authors and do not necessarily represent those of their affiliated organizations or those of the publisher, the editors, and the reviewers. Any product that may be evaluated in this article, or claim that may be made by its manufacturer, is not guaranteed or endorsed by the publisher.

Copyright © 2022 Cheng, Feng, Guo, Chen, Tan, Shi and Luo. This is an open-access article distributed under the terms of the Creative Commons Attribution License (CC BY). The use, distribution or reproduction in other forums is permitted, provided the original author(s) and the copyright owner(s) are credited and that the original publication in this journal is cited, in accordance with accepted academic practice. No use, distribution or reproduction is permitted which does not comply with these terms.